ORNL/TM-2022/2649

Safety Testing of AGR-5/6/7 Compacts 2-2-2 and 2-2-4

John D. Hunn
William F. Cureton
Darren J. Skitt
Fred C. Montgomery

September 2022

Approved for public release.
Distribution is unlimited.

OAK RIDGE National Laboratory

ORNL IS MANAGED BY UT-BATTELLE LLC FOR THE US DEPARTMENT OF ENERGY

ORNL/TM-2022/2649

Nuclear Energy and Fuel Cycle Division

SAFETY TESTING OF AGR-5/6/7 COMPACTS 2-2-2 AND 2-2-4

John D. Hunn
William F. Cureton
Darren J. Skitt
Fred C. Montgomery

September 2022

Work sponsored by
US DEPARTMENT OF ENERGY
Office of Nuclear Energy—Advanced Reactor Technologies
under the
Advanced Gas Reactor Fuel Development and Qualification Program

Prepared by
OAK RIDGE NATIONAL LABORATORY
Oak Ridge, TN 37831
managed by
UT-BATTELLE LLC
for the
US DEPARTMENT OF ENERGY
under contract DE-AC05-00OR22725

CONTENTS

LIST OF FIGURES

LIST OF TABLES

ABBREVIATIONS

AGR	Advanced Gas Reactor (Fuel Development and Qualification Program)
AGR-1	first AGR program irradiation experiment
AGR-2	second AGR program irradiation experiment
AGR-5/6/7	fifth, sixth, and seventh AGR program irradiation experiments
CCCTF	Core Conduction Cooldown Test Facility
EOI	end of irradiation
FIMA	fissions per initial metal atom
FITT	Furnace for Irradiated TRISO Testing
HTGR	high-temperature gas-cooled reactor
ID	identification
IFEL	Irradiated Fuels Examination Laboratory
JMOCUP	Jim's MCNP-ORIGEN2 coupled utility program
LBL	leach-burn-leach
MCNP	Monte Carlo N-Particle Transport code
ORIGEN	Oak Ridge Isotope Generation and Depletion code
ORNL	Oak Ridge National Laboratory
PIE	post-irradiation examination
SCR	silicon-controlled rectifier
SiC	silicon carbide (TRISO layer)
TA_{max}	time-average maximum (temperature)
TA_{min}	time-average minimum (temperature)
TAVA	time-average, volume-average (temperature)
TRISO	tristructural isotropic (coated particles)
UCO	uranium carbide and uranium oxide (fuel kernels)
UTC	Universal Time Coordinated

ACKNOWLEDGMENTS

This work was sponsored by the US Department of Energy, Office of Nuclear Energy, Advanced Reactor Technologies as part of the Advanced Gas Reactor Fuel Development and Qualification Program. Special thanks to the Irradiated Fuels Examination Laboratory Operations Group who were responsible for fuel transfers, furnace maintenance, and all in-cell manipulations for furnace operation and daily deposition cup changes. Special thanks also go to the Radiological Materials Analytical Laboratory's chemists (Chuck Watson for gamma spectrometry, Tamara Keever for mass spectrometry, Haley Wightman and Marc Chattin for sample preparation and radiochemistry, and Wade Ivey for data review) and radiological technicians (Lisa Duncan and John Garan), without whose support this work could not have been performed.

1. INTRODUCTION AND BACKGROUND

Compacts 2-2-2 and 2-2-4 from the Advanced Gas Reactor (AGR) Fuel Development and Qualification Program's final irradiation campaign (AGR-5/6/7) were each separately subjected to a thermal soak at 1600°C for 300 h under flowing helium to simulated conditions experienced during a postulated high-temperature gas-cooled reactor (HTGR) depressurization conduction cooldown event. The safety testing of the fuel compacts' performance under accident conditions was conducted in the Oak Ridge National Laboratory (ORNL) Core Conduction Cooldown Test Facility (CCCTF), which utilizes a stand-alone hot cell at the Irradiated Fuels Examination Laboratory (IFEL). The CCCTF heats fuel to temperatures up to 1900°C in a non-oxidizing environment while continuously monitoring the sweep gas for radioactive ^{85}Kr to detect release levels associated with hermetic failure of the tristructural-isotropic (TRISO) coating surrounding each fuel kernel. In addition, certain metallic radionuclides that escape the fuel compact are collected on deposition cups that are periodically exchanged with a new cup to obtain information on the overall retention behavior of the TRISO coating layers. Because cesium can diffuse through intact pyrocarbon layers, abnormal degradation of the silicon carbide (SiC) layer in the absence of holistic TRISO coating failure is indicated by release of ^{134}Cs at levels equivalent to an individual particle inventory in the absence of significant ^{85}Kr release (Hunn et al. 2014). Additional description of the CCCTF system is provided in Appendix A.

The thermal histories of the completed safety tests and results of the gamma analyses of metallic fission products (^{110m}Ag, ^{134}Cs, ^{137}Cs, ^{154}Eu, and ^{155}Eu) collected on the CCCTF water-cooled deposition cups and gaseous fission products (^{85}Kr) accumulated in the liquid nitrogen-cooled sweep gas trap are presented herein. Measured activities were decay corrected to July 23, 2020, at 7:10 Universal Time Coordinated (UTC), which corresponds to one day after the end of irradiation (EOI). Calculated compact inventories had previously been determined for one day after EOI, in which the one day was added to allow for decay of short-lived radionuclides (Sterbentz 2020). See Appendix B for the calculated values used for this report. Note that these calculated inventories do not account for any possible transport of actinides or fission products into or out of the fuel compacts during or after irradiation, they simply represent the net amount of each nuclide generated by the nuclear physics reactions occurring as a function of neutron interaction and time and not subsequently depleted by other nuclear physics reactions as of one day after EOI. The decay-corrected activity of each measured nuclide was divided by the calculated compact inventory of that nuclide to obtain the compact fraction deposited on each cup or accumulated in the sweep gas trap. It is also often useful to consider inventory values in terms of a particle equivalent value, which is calculated by multiplying the compact fraction by the estimated number of particles in the compact. The particle equivalent value provides insight when interpreting fission product release in relation to individual particle failure. For compacts from Capsule 2, the reported average of 2265 particles was used (Pham et al. 2021).

Fuel particles used in the AGR-5/6/7 irradiation experiment had properties similar to particles irradiated in the AGR program's second irradiation experiment (AGR-2), and both particle lots were fabricated by BWX Technologies Nuclear Operation Group. These particles contained kernels comprised of both uranium carbide and uranium oxide (UCO) and standard AGR TRISO coatings (Marshall 2020). Average irradiation conditions experienced by AGR-5/6/7 Compacts 2-2-2 and 2-2-4 during the 360.9 effective full power days of irradiation in the Advanced Test Reactor are given in Table 1-1. The compacts were irradiated with higher fast neutron fluences (neutron energies >0.18 MeV) and achieved higher burnups in percent fissions per initial metal atom (FIMA) than any of the AGR-2 UCO fuel compacts. However, the calculated temperatures during irradiation of AGR-5/6/7 Compacts 2-2-2 and 2-2-4 were notably lower than the range of temperatures explored in the AGR-2 UCO compact irradiations, which ranged from compact time-average, volume-average (TAVA) temperatures of 987°C–1296°C (Hawkes 2014). For context, the lowest localized time-average minimum (TA_{min}) temperature for an AGR-2 UCO compact was 868°C (AGR-2 Compact 6-4-3), and the localized time-average maximum (TA_{max}) temperature for an AGR-2 UCO compact was 1360°C (AGR-2 Compacts 2-3-1 and 2-3-2). These three AGR-2 compacts

that represent the temperature extremes of the AGR-2 UCO compact irradiation were subjected to safety testing in CCCTF during the AGR-2 post-irradiation examination (PIE) campaign, and results are available for comparison (Hunn et al. 2017, 2018a, 2019; Stempien et al. 2021).

Table 1-1. Irradiation conditions for AGR-5/6/7 Compacts 2-2-2 and 2-2-4

Compact ID [a]	Compact Batch ID [b]	Packing Fraction [b]	Approximate Number of Particles [b]	Burnup [c] (% FIMA)	Fast fluence [c] (n/m2)	Temperature [d] (°C)		
						TA_{min}	TAVA	TA_{max}
2-2-2	14156A	25.5%	2265	14.02	4.72×10^{25}	743	845	914
2-2-4	14156A	25.5%	2265	14.33	4.94×10^{25}	752	856	927

[a] The compact identification (ID) numbering convention of X-Y-Z denotes the compact's location in the irradiation test train: capsule-level-stack (Pham et al. 2021).
[b] Average compact batch properties data reported in the AGR-5/6/7 As-Run Report (Pham et al. 2021).
[c] Burnups and fast neutron fluences are based on physics calculations (Sterbentz 2020).
[d] Time-averaged irradiation temperatures are based on thermal calculations (Hawkes 2022).

2. 1600°C SAFETY TEST OF AGR-5/6/7 COMPACT 2-2-2

AGR-5/6/7 Compact 2-2-2 was the first AGR-5/6/7 safety test using the upgraded CCCTF controller (Cureton et al. 2022) and gamma spectrometry systems (Morris et al. 2022). Both upgrades replaced aging hardware and software that were no longer supported by the vendors with modern versions. The CCCTF upgrade also notably included the creation of an all-new graphical user interface using the National Instruments LabVIEW programming environment. The LabVIEW program controls and collects data from the furnace temperature control components, helium gas mass flow controllers, gas and vacuum system valves, and the components responsible for maintaining the temperature of the liquid nitrogen-cooled charcoal traps used to collect ^{85}Kr. Gamma detectors used to measure ^{85}Kr inventory in the traps are controlled by an independent gamma spectrometry system. The basic functionality of the CCCTF furnace and the liquid nitrogen-cooled charcoal trap system were unchanged by the upgrade, so data generated during safety testing remains consistent with that generated from the former 36 CCCTF safety tests of compacts from the first (AGR-1) and second (AGR-2) irradiation experiments.

Compact 2-2-2 was heated in flowing helium gas from room temperature to 400°C at 120°C/h, then held at 400°C for 2 h to promote removal of any residual moisture. Following the 400°C soak, heating resumed at 120°C/h until 1250°C was reached, then a 12 h soak at 1250°C was performed before proceeding to the safety test temperature of 1600°C at a reduced rate of 50°C/h. The first deposition cup was replaced near the end of the 1250°C soak, and the second deposition cup was replaced 1.5 h after reaching 1600°C. Less than 1 h after the second cup exchange, electrical power to the IFEL building was lost, which shutdown the high voltage furnace supply. Power to the CCCTF computer control system was preserved by the battery backup supply, so helium flow was maintained and temperature data continued to be collected at five-minute intervals (see Figure 2-1). After the power went out, the furnace cooled from 1600°C to 1215°C in less than 5 min at a rate of at least 77°C/min (normally, cooling rate is controlled to ≤10°C/min). The average cooling rate for the next two five-minute intervals was 56°C/min to 934°C and 38°C/min to 742°C. The furnace cooled from 742°C to 201°C in 30 min at average cooling rates between 29°C/min and 10°C/min over each five-minute interval. After this, the furnace cooled to 38°C at <10°C/min. Power was restored to the building about 1.5 h after the start of the outage. Because of the way the new furnace power supply silicon-controlled rectifier (SCR) and temperature controller had been configured, which has since been changed, the furnace began heating at the SCR power limit of 80% when power was restored. This caused the furnace to ramp to over 700°C at a rate of at least 135°C/min before the operator intervened. The furnace was cycled down to ~280°C and back up to 708°C over a period of 1 h, and then control was fully reestablished and the standard ramp rates of 120°C/h to 1250°C and 50°C/h to 1600°C were used to resume the safety test.

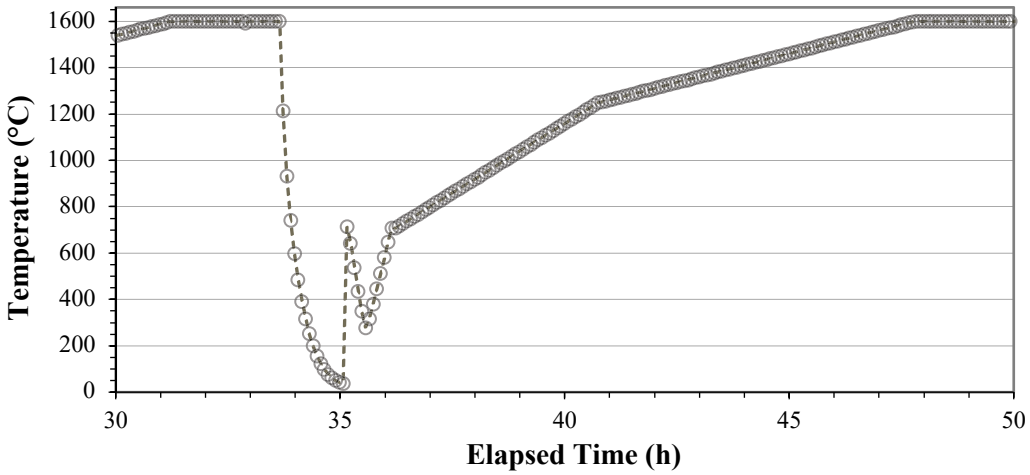

Figure 2-1. Temperature profile during AGR-5/6/7 Compact 2-2-2 safety test power outage event.

After returning to 1600°C, four deposition cups were replaced at intervals of ~12 h, and then the remaining cups were each allowed to reside in the furnace for ~24 h. A shorter exchange period is used at the beginning of a safety test to better capture the time dependence of fission product release during the period when silver release rates are often the highest and when cesium release from any preexisting or early particle failure would occur. The markers in Figure 2-2 show the time since the start of the test that each cup was removed and the compact fraction of five commonly tracked gamma-emitting radionuclides measured on each cup. Figure 2-3 shows the same data, but the cup activities are plotted in terms of the average collection rate (i.e., the measured compact fraction divided by the cup residence time).

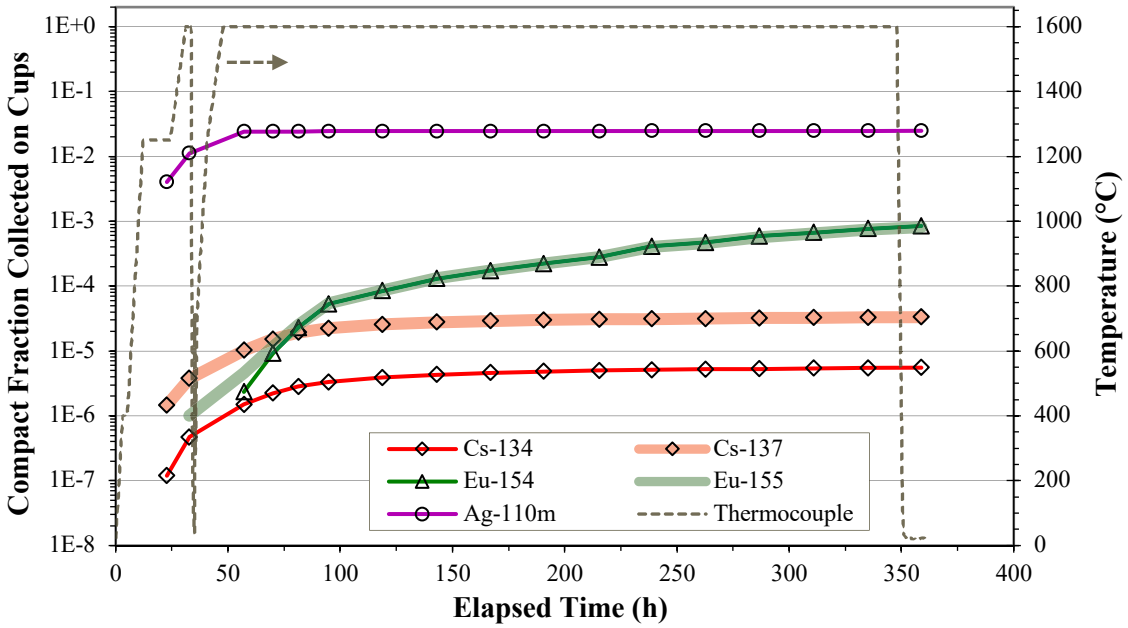

Figure 2-2. Cumulative accumulation of metallic fission products on deposition cups during 1600°C safety test of AGR-5/6/7 Compact 2-2-2.

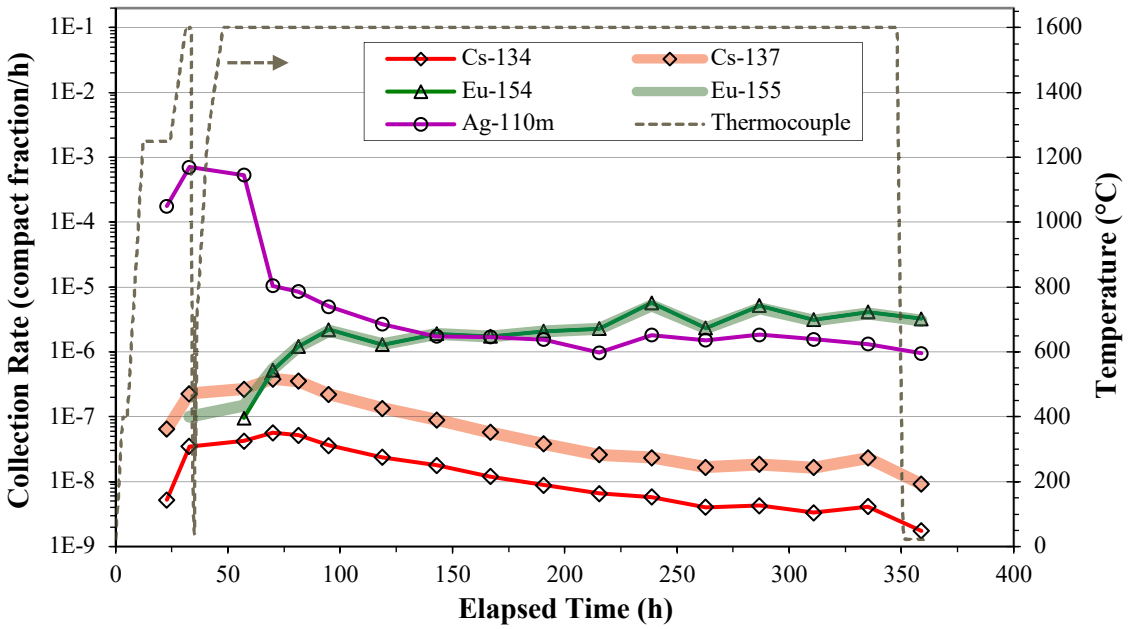

Figure 2-3. Rate of accumulation of metallic fission products on deposition cups during 1600°C safety test of AGR-5/6/7 Compact 2-2-2.

Radionuclide release during the 1600°C safety test of Compact 2-2-2 showed typical behavior for an AGR safety test of a compact containing no particles with compromised SiC layers, and there was no indication that the higher-than-normal rate of thermal cycling surrounding the power outage had any adverse effect on TRISO particle performance. First, there was no measurable activity from ^{85}Kr detected in the liquid nitrogen-cooled sweep gas trap. The minimum detection limit for ^{85}Kr was estimated to be <0.02 μCi, which corresponds to <0.0013 particle equivalents. As such, it can be concluded that no particles in the compact experienced TRISO failure, which would have resulted in release of gaseous fission products and detection of significantly more ^{85}Kr in the sweep gas trap (Demkowicz et al. 2015).

Second, there was no indication of excessive cesium release from Compact 2-2-2 that would indicate the presence of particles with failed SiC. The cumulative compact fraction of ^{134}Cs collected on the deposition cups was 5.5E-6 (0.013 particle equivalents). Cumulative ^{134}Cs release during 1600°C safety testing of three separate AGR-1 compacts that each contained a single failed particle was much higher at 0.49, 0.69, and 0.89 particle equivalents (Hunn et al. 2014). There were no observed SiC failures during 1600°C safety testing of AGR-2 UCO compacts. In the absence of excessive contamination from sources external to the compact, cumulative ^{134}Cs release from AGR-2 compacts after 300 h at 1600°C was 0.0008–0.024 particle equivalents (Stempien et al. 2021). Release from AGR-5/6/7 Compact 2-2-2 was consistent with the AGR-2 results. Figure 2-3 shows that the ^{134}Cs and ^{137}Cs collection rates peaked within the first 24 h at 1600°C and dropped off steadily thereafter. This behavior is consistent with removal of ^{134}Cs and ^{137}Cs contamination that may be introduced when the compact, graphite holder, deposition cups, cold finger, or other CCCTF furnace internals are exposed within the hot cell (a new tantalum container and tantalum sweep gas tube are installed in the furnace before starting each test to minimize cross contamination between tests). The locations of these components within the furnace are shown in Appendix Figure A-1. Further evidence that the ^{134}Cs and ^{137}Cs measurements were dominated by hot cell contamination comes from the higher observed compact fraction of ^{137}Cs. Figure 2-2 and Figure 2-3 show similar time dependent behavior for ^{134}Cs and ^{137}Cs, as expected for two isotopes of the same element, but the compact fraction of ^{137}Cs was consistently higher. This can be explained by the relatively higher inventory of ^{137}Cs present as general contamination inside the IFEL hot cells. Given the relatively greater contribution from hot cell contamination to the measured ^{137}Cs activity, the measured ^{134}Cs values represent a better upper bound on the cesium associated with the fuel in the compact under test.

Europium behavior was monitored by measuring the gamma emissions from ^{154}Eu and ^{155}Eu. Unlike ^{134}Cs and ^{137}Cs, Figure 2-2 and Figure 2-3 show that these two europium isotopes overlap when plotted in terms of the compact fraction. This indicates that the observed ^{154}Eu and ^{155}Eu values were mostly originating from the fuel compact. The cumulative compact fraction of ^{154}Eu collected on the deposition cups was 8.5E-4 (1.9 particle equivalents), which was 153× higher than ^{134}Cs. This indication for higher release of europium was not unexpected, given that europium has been noted to diffuse more readily through intact SiC compared with cesium, and europium is better retained in the compact matrix while the compact is in the reactor (Hunn et al. 2018b).

Figure 2-3 shows that the average rates at which ^{154}Eu and ^{155}Eu were deposited on the cups increased over the first 48 h at 1600°C and then held relatively constant. This behavior has been observed throughout AGR-1 and AGR-2 safety testing and is associated with the relatively slower transport of europium out of the compact, through the graphite holder, and to the cups, compared with the more volatile species of cesium and silver. While ^{134}Cs and ^{137}Cs collection rates dropped off throughout the safety test as the source of available cesium was depleted, the relatively constant collection rates of ^{154}Eu and ^{155}Eu indicate that a significant fraction of what was released was still available for transport to the cups at the end of the 300 h soak. At the end of the safety test, ^{154}Eu in the graphite holder was measured by oxidizing the holder in air at 750°C and dissolving europium oxide in hot nitric acid for mass spectrometry. The compact fraction of ^{154}Eu in the graphite holder was 4.7E-3, which was 5.5× the cumulative amount collected on the cups. Significant activity from ^{154}Eu was also observed on the

tantalum furnace internals. Additional post-safety test acid leaching of the tantalum internals will provide the remaining data needed to quantify the total ^{154}Eu release from the compact. As AGR-5/6/7 PIE progresses, leach-burn-leach (LBL) analysis of AGR-5/6/7 Compacts 2-2-2 and 2-2-4 will provide data on how much ^{154}Eu and ^{155}Eu remained after safety testing in the graphitic matrix and outer pyrocarbon layers within each compact (i.e., outside of intact SiC layers), and this data in conjunction with the safety test data will be compared to LBL data from similar as-irradiated compacts to estimate how much ^{154}Eu and ^{155}Eu diffused through intact SiC during the 1600°C safety test.

The cumulative compact fraction of ^{110m}Ag collected on the deposition cups during the Compact 2-2-2 safety test was 2.48E-2 (56 particle equivalents). Most of the ^{110m}Ag was collected on the first three cups, as shown in Table 2-1. Only 2.9% of the cumulative amount of ^{110m}Ag measured on the deposition cups was collected during the latter 290.6 h of the 302.5 h at 1600°C. This is common behavior that has been observed throughout AGR-1 and AGR-2 safety testing (Demkowicz et al. 2015; Stempien et al. 2021). The ^{110m}Ag collected during these early stages of the AGR-5/6/7 Compact 2-2-2 safety test came from ^{110m}Ag released through intact SiC layers during irradiation that was retained within the compact at the end of irradiation as well as ^{110m}Ag released through intact SiC during the safety test, especially as the compact temperature passed through a temperature zone where enhanced silver release has been observed. In one study, silver release was observed to be higher at temperatures between 1075°C and 1375°C than at 1450°C and 1600°C (Hunn et al. 2015). This phenomenon is currently under study using particles from AGR-5/6/7 Compact 2-2-1, which are being heated in the ORNL Furnace for Irradiated TRISO Testing (FITT) at 100°C increments from 1100°C to 1600°C. The FITT study using AGR-5/6/7 particles is a follow-on from a previous study of AGR-2 particles whose ^{110m}Ag inventory had decayed over more than 6.3 ^{110m}Ag half-lives to a point were measurement uncertainty obscured conclusive observation of a reduction in ^{110m}Ag inventory within each particle (Gerczak 2020). The AGR-5/6/7 particles are being studied earlier in the AGR-5/6/7 PIE campaign, and the study will be completed before 3.2 ^{110m}Ag half-lives have passed. Previous CCCTF safety tests that had unplanned interrupted heating profiles have exhibited evidence for additional ^{110m}Ag release when the compacts were ramped back to the safety test temperature. It is likely that some of the ^{110m}Ag collected on Cup 3 included this additional release due to the thermal cycling. This effect was more evident during the AGR-5/6/7 Compact 2-2-4 safety test, as discussed in Section 3.

Table 2-1. Collection of ^{110m}Ag on deposition cups early in the 1600°C safety test of AGR-5/6/7 Compact 2-2-2

Cup Number	Temperature (°C)	Compact Fraction	Particle Equivalent	Fraction of Total
1	22–1250	4.03E-3	9.1	16.3%
2	1250–1600	7.11E-3	16.1	28.7%
3	1600–38–1600	1.29E-2	29.3	52.1%

* Only 2.9% of the cumulative amount of ^{110m}Ag measured on the deposition cups was collected during the latter 290.6 h of the 302.5 h at 1600°C.

3. 1600°C SAFETY TEST OF AGR-5/6/7 COMPACT 2-2-4

The AGR-5/6/7 Compact 2-2-4 safety test was performed shortly after completion of the Compact 2-2-2 safety test using the same planned heating profile. However, two unplanned interruptions occurred. As for Compact 2-2-2, Compact 2-2-4 was heated in flowing helium gas from room temperature to 400°C at 120°C/h, held 2 h at 400°C, heated to 1200°C at 120°C/h, held 12 h at 1250°C, heated at 50°C/min to 1600°C, and held at 1600°C with the intention of soaking for 300 h. The first deposition cup was replaced near the end of the 1250°C soak and the Cup 2 was replaced soon after reaching 1600°C. Cups 3–5 were replaced at intervals of ~12 h, after which the cup exchange period transitioned to daily. However, after Cup 6 was removed from the cold finger and Cup 7 attached for insertion into the furnace, problems with uncontrolled cold finger movement outside the furnace prompted the operator to activate the system emergency stop, which stopped the cold finger, but also cut off the furnace. Power to the computer was maintained, so temperature data continued to be logged at five-minute intervals, except for the 38 min when the furnace was cooling from 767°C to 278°C because operators restarted the system during the effort to restore cold finger control. Figure 3-1 shows the temperatures recorded during the thermal transient. The furnace cooled from 1600°C to 1225°C at a rate of at least 75°C/min. The average cooling rates for the next two five-minute periods were 57°C/min to 937°C and 34°C/min to 767°C. These cooldown rates were similar to those observed during the initial 15 min following the Compact 2-2-2 safety test power failure discussed in Section 2. It took 76 min for the furnace to cool from 934°C to 38°C following the Compact 2-2-2 safety test power failure, while it took 84 min for the furnace to cool from 937°C to 39°C following the first Compact 2-2-4 safety test shutdown. The minor difference in cooling rates may have been related to the fact that the cold finger was in the furnace during the Compact 2-2-2 power failure event, while during the first furnace shutdown of the Compact 2-2-4 safety test, the cold finger was out of the furnace, the airlock gate valve was closed, and the thermal shields were swung in place between the internal hot zone and the gate valve. These components are described in Appendix A and shown in Appendix Figure A-1.

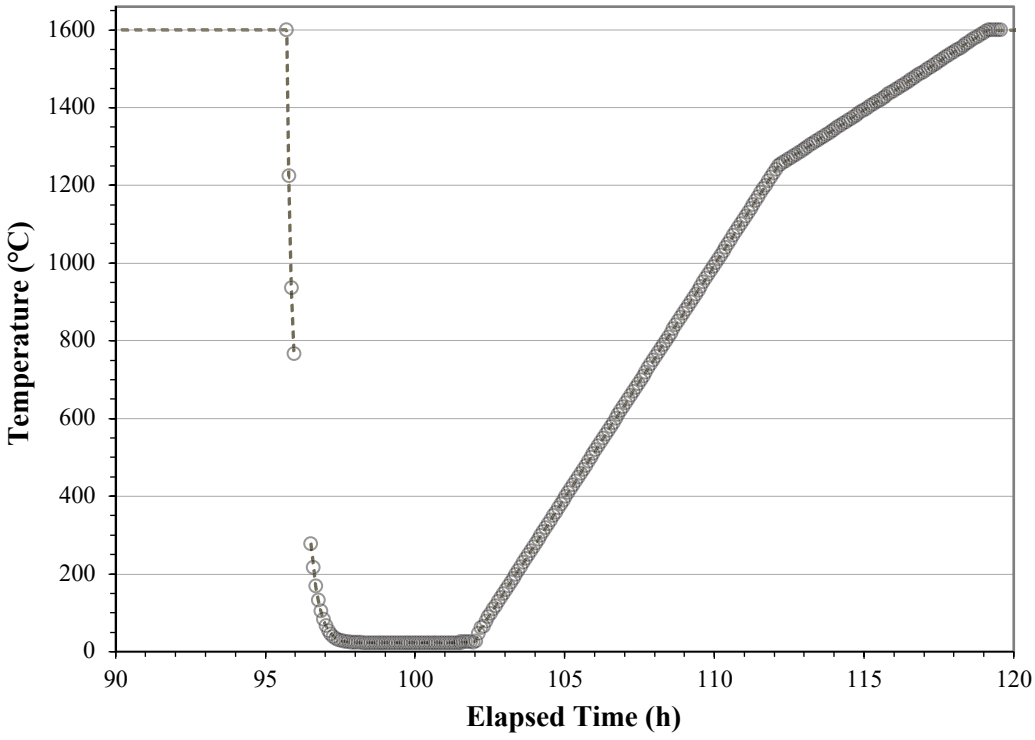

Figure 3-1. Recorded temperatures during first unplanned thermal cycle of AGR-5/6/7 Compact 2-2-4 (27 h pause at room temperature not shown).

The next day, the safety test was resumed using the normal heating rates to return to 1600°C (see Figure 3-1). Cup 7 was replaced 0.5 h after the furnace reached 1600°C to assess for any unusual fuel failure associated with the first unplanned thermal cycle, and none was observed. Cup 8 was replaced without trouble, but another issue with uncontrolled cold finger movement occurred during the Cup 9 removal. Cold finger travel did not halt at the air lock interlock position when the cold finger was being raised out of the furnace. Under normal operation, the cold finger stops here so that the thermal shields can be swung into position and the gate vale closed. Instead, the cold finger continued travelling upward past this point and the cup was observed to partially exit the spool piece at the top of the air lock. The cold finger movement was halted manually by engaging the cold finger stop switch and the furnace placed in a safe condition by swinging in the thermal shields and closing the gate valve. The LabVIEW software continued to collect temperature data for about 10 min and then froze. As designed, the temperature controller continued to operate when the LabVIEW software froze, so the furnace was maintained at 1600°C. Rebooting the computer required temporary shutdown of the furnace power supply SCR for about 12 min, after which the furnace was manually reheated to 1530°C while the software issue was being diagnosed. After about an hour of unsuccessful efforts to restore computer control, the decision was made to temporarily halt the test until the computer failure could be addressed and additional manual cold finger controls added to the system to prevent reoccurrence of the cold finger movement problems experienced during this safety test. Figure 3-2 shows a portion of the period of manual temperature control, which was recorded in a cell phone video. The average rate of recorded temperature change was <40°C/min, and rates reached as high as 70°C–100°C for about 3 min during the 17 min period recorded by video.

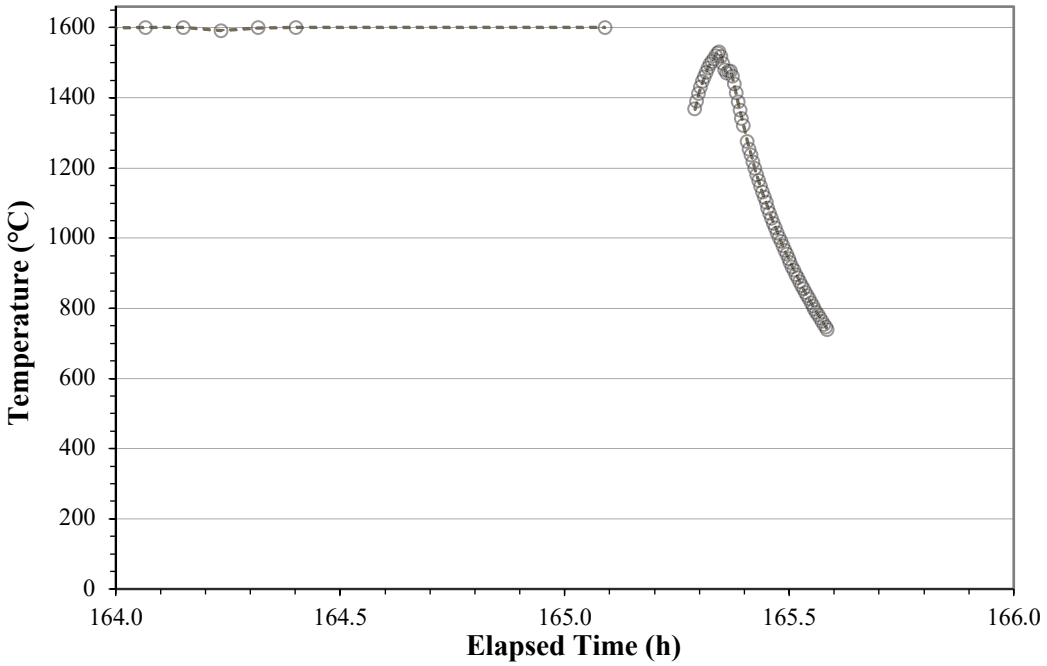

Figure 3-2. Temperature profile during second unplanned thermal cycle of AGR-5/6/7 Compact 2-2-4.

The safety test was paused for eleven days. Over this period, the computer and software issues were addressed, hardware modifications for manual cold finger control were installed, and the gate valve O-ring was replaced because it had been compromised by excess heat while thermal shields were out of position. The safety test was resumed using the normal heating rates to return to 1600°C. Because the fuel compact had been removed from the furnace to replace the gate valve O-ring and visually inspect the furnace interior, a hold at 400°C for 2 h was included in the heating schedule to promote removal of any moisture, as is done at the start of all safety tests. Cup 10 was replaced when the furnace reached 1600°C, and the remainder of the safety test was completed as planned.

As was observed for the 1600°C safety test of Compact 2-2-2, the unplanned furnace shutdowns during the Compact 2-2-4 safety test at 1600°C showed no indication of any adverse effect from the thermal cycling on particle performance (Figure 3-3). There was no measurable activity from ^{85}Kr detected in the sweep gas trap (<0.0013 particle equivalents), which indicated no particles in Compact 2-2-4 experienced TRISO failure. There was also no indication of excessive cesium release that would indicate the presence of particles with failed SiC. The cumulative compact fraction of ^{134}Cs collected on the deposition cups was 5.7E-6 (0.013 particle equivalents). This was nearly the same amount of ^{134}Cs collected during the Compact 2-2-2 safety test. See the discussion in Section 2 comparing this level of release to AGR-1 and AGR-2 safety testing. Figure 3-4 shows that the average rates of ^{134}Cs and ^{137}Cs collection over each cup residence period during the Compact 2-2-4 safety test peaked within the first 24 h at 1600°C. Like the Compact 2-2-2 safety test, ^{137}Cs showed the same time-dependent behavior as ^{134}Cs, but the measured compact fraction was consistently higher. As discussed in Section 2, it can be concluded that the measured ^{137}Cs was dominated by hot cell contamination and the measured ^{134}Cs represents an upper bound on the cesium associated with the fuel in the compact. The declining rate of cesium collection after the first 24 h at 1600°C indicates that diffusion of cesium through the particles' SiC layers was negligible compared with the total release. Dips in the average ^{134}Cs and ^{137}Cs collection rates shown in Figure 3-4 for Cups 7 and 10 were a result of the relatively shorter fraction of their residence time spent at elevated temperature, compared with the preceding and succeeding cups that spent all their time in the furnace at 1600°C.

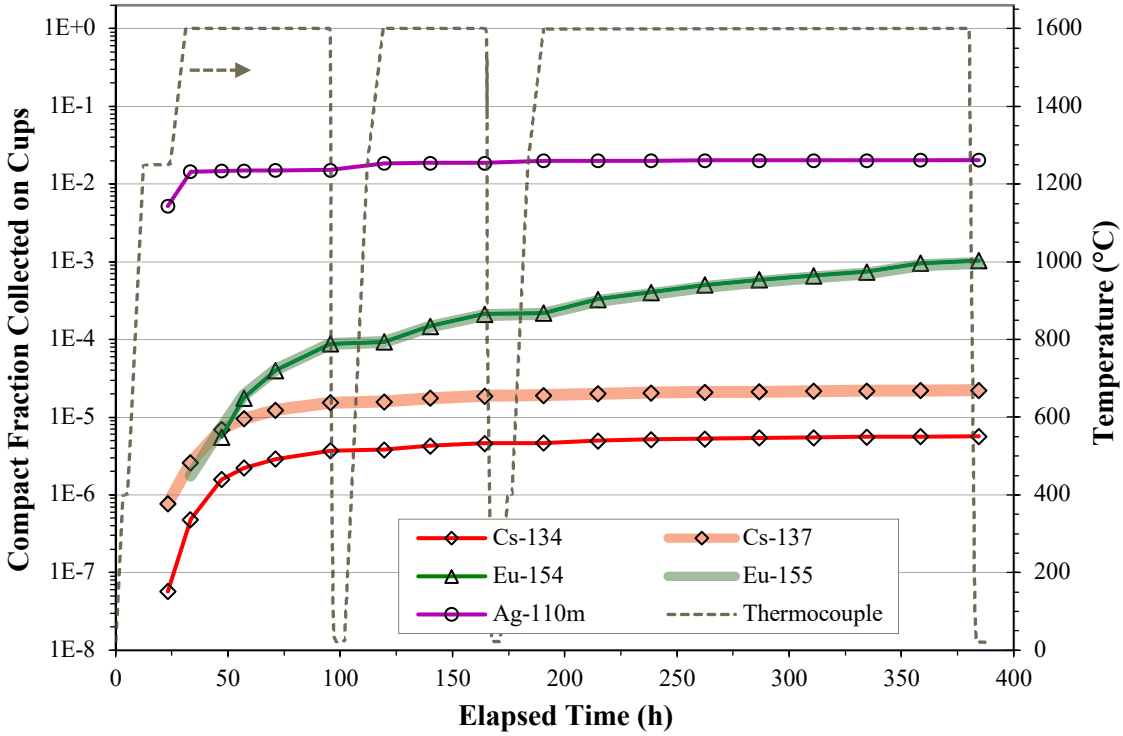

Figure 3-3. Cumulative accumulation of metallic fission products on deposition cups during 1600°C safety test of AGR-5/6/7 Compact 2-2-4.

The average ^{154}Eu and ^{155}Eu collection rates shown in Figure 3-4 for Cups 7 and 10 also show dips compared with preceding and succeeding cups due to limited residence time at 1600°C. Disregarding these dips associated with the lower temperature periods, the ^{154}Eu and ^{155}Eu collection data for the Compact 2-2-2 and Compact 2-2-4 safety tests were similar. The ^{154}Eu and ^{155}Eu collection rates peaked later than ^{134}Cs and ^{137}Cs due to relatively slower transport to the cups, as discussed in Section 2. In both tests, ^{154}Eu and ^{155}Eu collection rates were fairly constant after Cup 6, indicating significant europium remained in the graphite holder. The cumulative compact fraction of ^{154}Eu collected on the deposition

cups by the end of the Compact 2-2-4 safety test was 1.04E-3 (2.3 particle equivalents), compared with 8.5E-4 (1.9 particle equivalents) at the end of the Compact 2-2-2 safety test. These values suggest similar behavior, but more rigorous comparison might be possible after a mass balance analysis of all the ^{154}Eu and ^{155}Eu released from the compacts. As discussed for Compact 2-2-2 in Section 2, post-safety test analysis of the graphite holder and tantalum internals from the Compact 2-2-4 safety test will provide the data needed for this mass balance.

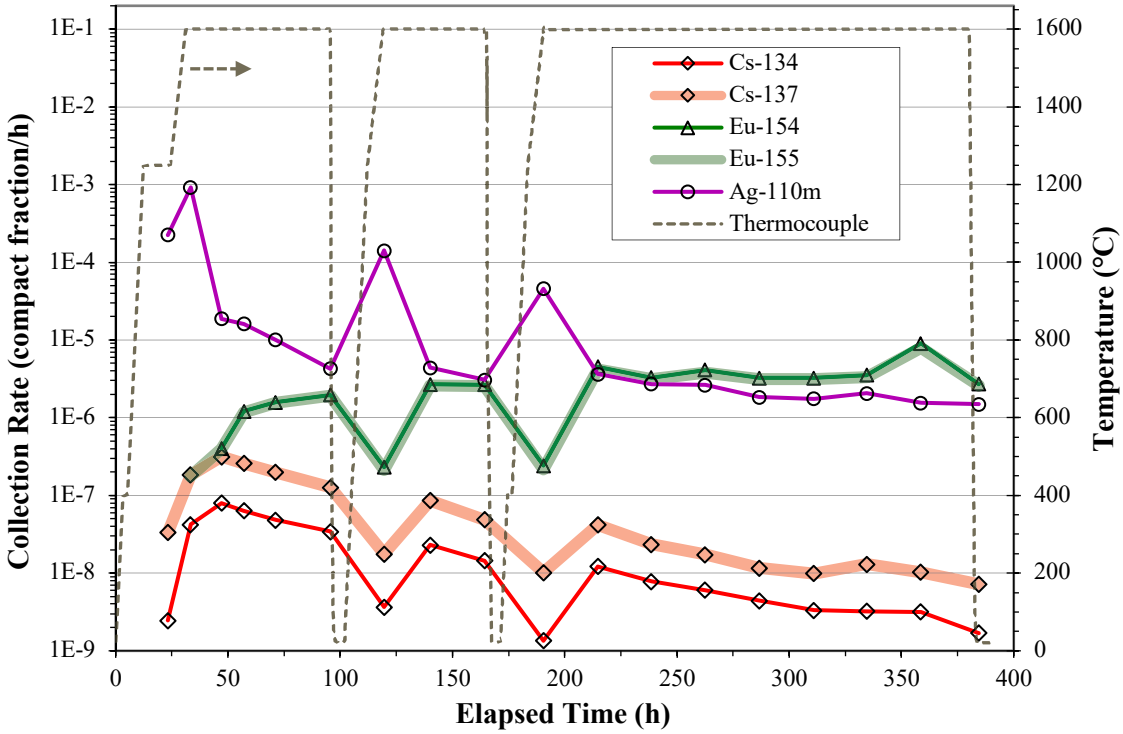

Figure 3-4. Rate of accumulation of metallic fission products on deposition cups during 1600°C safety test of AGR-5/6/7 Compact 2-2-4.

The cumulative compact fraction of ^{110m}Ag collected on the deposition cups during the Compact 2-2-4 safety test was 2.03E-2 (46 particle equivalents). The maximum collection rates for ^{110m}Ag occurred during the periods of slowly heating the compact through the 1075°C–1375°C zone in which enhanced diffusion is thought to occur, as discussed in Section 2. Table 3-1 shows the amounts of ^{110m}Ag collected on the four cups residing in the furnace during these periods. These four cups accounted for 93.8% of the cumulative collected ^{110m}Ag. The ^{110m}Ag collected on the first two cups presumably came from ^{110m}Ag released through intact SiC layers during irradiation that was retained within the compact at the end of irradiation as well as ^{110m}Ag released through intact SiC during the thermal ramp to 1600°C. However, the steadily decreasing ^{110m}Ag collection rates for Cups 3–6 indicate that the exposed ^{110m}Ag from the irradiation test was mostly depleted from the compact by the time Cup 2 was removed (~2 h after reaching 1600°C for the first time) and any diffusional release through intact SiC at 1600°C was relatively low. Therefore, the ^{110m}Ag collected on Cup 7, which was removed ~30 min after returning to 1600°C at the end of the first unplanned thermal cycle, can be presumed to have been predominately from enhanced diffusion through intact SiC at temperatures below 1600°C (Hunn et al. 2015). The same conclusion can be drawn from the observed spike in ^{110m}Ag collection rate for Cup 10, which was removed <5 min after returning to 1600°C at the end of the second unplanned thermal cycle, because the low ^{110m}Ag activities on Cups 8 and 9 indicated ^{110m}Ag had again been depleted prior to the start of the second unplanned shutdown.

Table 3-1. Collection of ^{110m}Ag during periods of thermal ramping in the AGR-5/6/7 Compact 2-2-4 safety test

Cup Number	Temperature (°C)	Compact Fraction	Particle Equivalent	Fraction of Total
1	22–1250	5.22E-3	11.8	25.7%
2	1250–1600	9.27E-3	21.0	45.6%
7	26–1600	3.38E-3	7.7	16.6%
10	22–1600	1.20E-3	2.7	5.9%

* Only 6.2% of the cumulative amount of collected ^{110m}Ag was measured on the other 14 deposition cups.

4. SUMMARY

The first two ORNL CCCTF safety tests on AGR-5/6/7 compacts were completed in fiscal year 2022. These were also the first two tests in the CCCTF using a new control system designed and installed in 2022. AGR-5/6/7 Compacts 2-2-2 and 2-2-4 were each heated in flowing helium gas at 1600°C for a total time of ~300 h while monitoring for time-dependent release of ^{85}Kr and metallic fission products. The Compact 2-2-2 safety test included an unplanned thermal cycle caused by a power outage. While such outages are typically unavoidable, the power outage revealed an issue with the configuration of the new control system that caused a higher-than-desired heating rate when power was restored. The system has been reconfigured to provide a rate-controlled resumption of a safety test after a power outage. The Compact 2-2-4 safety test included two unplanned thermal cycles. These were both related to intermittent issues with computer-control of the cold finger travel that did not manifest during the shakedown testing of the new CCCTF control system. Manual controls and a higher level of operator involvement in the process have been implemented as an immediate solution to the cold finger control problem experienced during this test, and other modifications are being considered.

The ^{85}Kr and ^{134}Cs releases from AGR-5/6/7 Compacts 2-2-2 and 2-2-4 were consistent with the previously observed performance of all six AGR-2 UCO fuel compacts safety tested at 1600°C, in which no particles exhibited failed TRISO or failed SiC (Stempien et al. 2021). After 300 h at 1600°C, the cumulative ^{85}Kr releases from AGR-5/6/7 Compacts 2-2-2 and 2-2-4 were well below a level that would signify the presence of a particle with failed TRISO. Cumulative ^{134}Cs releases were well below what have been observed in 1600°C safety testing of AGR-1 compacts containing particles with significant degradation of the normal retentive properties of the SiC (Hunn et al. 2014). It is notable that the higher than planned heating and cooling rates both AGR-5/6/7 Compacts 2-2-2 and 2-2-4 experienced during unplanned interruptions of the 1600°C safety test soak did not adversely impact the failure fractions.

Europium releases were higher than cesium releases, as expected from previous AGR safety testing (Demkowicz et al. 2015; Stempien et al. 2021). Although measured levels were equivalent to the calculated inventory in several particles, the absence of significant cesium releases indicated that the observed ^{154}Eu and ^{155}Eu was not from failed particles. Europium release during irradiation and safety testing is understood to typically come from most if not all of the particles in the compact, due to diffusion through the TRISO coatings. As discussed in Sections 2 and 3, the amount of ^{154}Eu and ^{155}Eu measured on the deposition cups only represented a minor fraction of what was released from the compact and data from additional post-safety test analyses are needed to quantify the releases. Because the time for transport of europium to the deposition cups was long compared with the cup exchange periods, the time dependencies in the cup collection data for ^{154}Eu and ^{155}Eu presented in Sections 2 and 3 are not accurate indicators of the time-dependent releases of ^{154}Eu and ^{155}Eu from the fuel compacts.

Silver releases during safety testing of AGR-5/6/7 Compacts 2-2-2 and 2-2-4 were also consistent with previous AGR testing (Morris et al. 2014; Hunn et al. 2018b). Almost all of the ^{110m}Ag released through intact SiC during irradiation, but still retained in the compacts at the end of the irradiation test, was released from AGR-5/6/7 Compacts 2-2-2 and 2-2-4 near the beginning of the safety tests. The unplanned thermal cycling during the Compact 2-2-4 safety test, which occurred after this initial release of ^{110m}Ag and when the ^{110m}Ag release rates were low, showed clear evidence for additional ^{110m}Ag release as a result of the thermal cycling. This additional release was consistent with previous observations of higher ^{110m}Ag release at temperatures between 1075°C and 1375°C compared with release at 1450°C and 1600°C (Hunn et al. 2015).

5. REFERENCES

Croff, Allen G. 1983. "ORIGEN2: A Versatile Computer Code for Calculating the Nuclide Compositions and Characteristics of Nuclear Materials." *Nucl. Tech.* 62: 335–352

Cureton, William F., Ricardo E. Muse, David A. Wilson, Robert N. Morris, and John D. Hunn. 2022. *Upgrade of Core Conduction Cooldown Test Facility Control System*. ORNL/LTR-2022/19. Oak Ridge: Oak Ridge National Laboratory.

Demkowicz, Paul A., Edward L. Reber, Dawn M. Scates, Les Scott, and Blaise P. Collin. 2015. "First High Temperature Safety Tests of AGR-1 TRISO Fuel with the Fuel Accident Condition Simulator (FACS) Furnace." *J. Nucl. Mater.* 464: 320–330.

Demkowicz, Paul A., John D. Hunn, Robert N. Morris, Isabella J. van Rooyen, Tyler J. Gerczak, Jason M. Harp, and Scott A. Ploger. 2015. *AGR-1 Post Irradiation Examination Final Report*. INL/EXT-15-36407. Idaho Falls: Idaho National Laboratory.

Gerczak, Tyler J., Zachary M. Burns, Darren J. Skitt, Robert N. Morris, and John D. Hunn. 2020. *AGR-2 Loose Particle Heating Tests in the Furnace for Irradiated TRISO Testing*. ORNL/TM-2020/1715. Oak Ridge: Oak Ridge National Laboratory.

Hawkes, Grant L. 2014. *AGR-2 Daily As-Run Thermal Analyses.* INL/ECAR-2476, Revision 1. Idaho Falls: Idaho National Laboratory.

Hawkes, Grant L. 2022. *AGR-5/6/7 Daily As-Run Thermal Analyses*. ECAR-5633. Idaho Falls: Idaho National Laboratory.

Hunn, John D., Charles A. Baldwin, Tyler J. Gerczak, Fred C. Montgomery, Robert N. Morris, Chinthaka M. Silva, Paul A. Demkowicz, Jason M. Harp, Scott A. Ploger, Isabella J. van Rooyen, and Karen E. Wright. 2014. "Detection and Analysis of Particles with Failed SiC in AGR-1 Fuel Compacts." *Proceedings of the 7th International Topical Meeting on High Temperature Reactor Technology (HTR-2014)*. Weihai, October 27–31, 2014. Also published in *Nucl. Eng. Des.* 360: 36–46.

Hunn, John D., Robert N. Morris, Charles A. Baldwin, Fred C. Montgomery, and Tyler J. Gerczak. 2015. *PIE on Safety-Tested AGR-1 Compact 4-2-2*. ORNL/TM-2015/033. Oak Ridge: Oak Ridge National Laboratory.

Hunn, John D., Robert N. Morris, Charles A. Baldwin, Zachary M. Burns, Fred C. Montgomery, and Darren J. Skitt. 2017. *Safety Testing of AGR-2 UCO Compacts 6-4-2 and 2-3-1*. ORNL/TM-2017/439. Oak Ridge: Oak Ridge National Laboratory.

Hunn, John D., Robert N. Morris, Fred C. Montgomery, Tyler J. Gerczak, Darren J. Skitt, Grant W. Helmreich, Brian D. Eckhart, and Zachary M. Burns. 2018a. *Safety Testing and Post-Safety-Test Examination of AGR-2 UCO Compact 2-3-2 and AGR-2 UO_2 Compact 3-4-1*. ORNL/TM-2018/956. Oak Ridge: Oak Ridge National Laboratory.

Hunn, John D., Robert N. Morris, Fred C. Montgomery, Tyler J. Gerczak, Darren J. Skitt, Charles A. Baldwin, John A. Dyer, Grant W. Helmreich, Brian D. Eckhart, Zachary M. Burns, Paul A. Demkowicz, and John D. Stempien. 2018b. "Post-Irradiation Examination and Safety Testing of US AGR-2 Irradiation Test Compacts." *Proceedings of the 9th International Topical Meeting on High Temperature Reactor Technology (HTR-2018)*. Warsaw, October 8–10, 2018.

Hunn, John D., Tyler J. Gerczak, Robert N. Morris, Fred C. Montgomery, Darren J. Skitt, Brian D. Eckhart, and Zachary M. Burns. 2019. *Safety Testing and Destructive Examination of AGR-2 UCO Compact 6-4-3*. ORNL/TM-2019/1200. Oak Ridge: Oak Ridge National Laboratory.

Ludwig, Scott B., and Allen G. Croff. 2002. *ORIGEN2.2—Isotope Generation and Depletion Code Matrix Exponential Method*. Oak Ridge: Oak Ridge National Laboratory.

Marshall, Douglas W. 2020. *AGR-5/6/7 Fuel Fabrication Report*. INL/EXT-19-53720. Idaho Falls: Idaho National Laboratory.

Morris, Robert N., and Charles A. Baldwin. 2010. *AGR CCCTF Calibration for Krypton-85 Activity Determination*. ORNL/TM-2010/180. Oak Ridge: Oak Ridge National Laboratory.

Morris, Robert N., Charles A. Baldwin, Paul A. Demkowicz, Hunn, John D., and Edward L. Reber. 2014. "Performance of AGR-1 High-Temperature Reactor Fuel During Post-Irradiation Heating Tests." *Proceedings of the 7th International Topical Meeting on High Temperature Reactor Technology (HTR-2014)*. Weihai, October 27–31, 2014. Also published in *Nucl. Eng. Des.* 360: 24–35.

Morris, Robert N., Darren J. Skitt, Charles A. Baldwin, and John D. Hunn. 2022. *Upgrade of Gamma Spectrometry Systems for ORNL TRISO Fuel PIE*. ORNL/TM-2021/2357. Oak Ridge: Oak Ridge National Laboratory.

Pham, Binh T., Joe J. Palmer, Douglas W. Marshall, James W. Sterbentz, Grant L. Hawkes, and Dawn M. Scates. 2021. *AGR-5/6/7 Irradiation Test Final As-Run Report*. INL/EXT-21-64221. Idaho Falls: Idaho National Laboratory.

Stempien, John D., John D. Hunn, Robert N. Morris, Tyler J. Gerczak, and Paul A. Demkowicz. 2021. *AGR-2 TRISO Fuel Post-Irradiation Examination Final Report*. INL/EXT-21-64279. Idaho Falls: Idaho National Laboratory.

Sterbentz, James W. 2020. *JMOCUP Physics Depletion Calculations for the As-Run AGR-5/6/7 TRISO Particle Experiment in ATR Northeast Flux Trap*. ECAR-5321. Idaho Falls: Idaho National Laboratory.

X-5 Monte Carlo Team. 2003. *MCNP—A General Monte Carlo N-Particle Transport Code.* Version 5, Volume I (LA-UR-03-1987) and Volume II (LA-CP-03-0245). Los Alamos: Los Alamos National Laboratory.

APPENDIX A. CCCTF FURNACE AND TRAP SYSTEMS*

The CCCTF was developed at ORNL in the early 1990s to perform high temperature accident simulation performance tests on coated particle fuels. The system has undergone several modifications and now consists of a water-cooled graphite resistance heated tube furnace in a vertical orientation with an internal tantalum container that isolates the test specimens from the furnace heating elements. A helium sweep gas system provides the test atmosphere and transports released fission gases to a cryogenic trap system for collection and gamma counting. Water cooling circuits provide temperature control for sensitive furnace components (including the metal furnace jacket and the cold finger). The furnace system diagram is shown in Appendix Figure A-1, and a photograph of the furnace is shown in Appendix Figure A-2.

Fuel specimens are housed in a graphite or refractory metal holder that is loaded from the top prior to the start of the run and rests on the bottom of the tantalum container. An inverted well at the bottom of the tantalum container protrudes into the center of the sample holder. A dual Type C thermocouple inside the well serves to measure the sample temperature and provide an input for the furnace control system. The temperature of the tantalum container can also be monitored from the outside through a furnace window using an optical pyrometer. A copper-plated steel deposition cup is attached to the bottom of a water-cooled cold finger by means of a screw mechanism and acts as the collection surface for condensable metallic fission products. The deposition cup is periodically exchanged with a new cup to obtain a time-dependent history of the metallic nuclide releases. Radiochemical analyses (gamma, beta, and mass spectrometry) provide quantification of the collected nuclides.

To exchange deposition cups, the cold finger is inserted and removed from the top through an air lock while the fuel is held at temperature. When the cold finger is being removed from the furnace, thermal shields are manually swung into place to minimize heating of the gate valve assembly, then the gate valve is closed to maintain the helium atmosphere in the tantalum can before the cold finger is removed through the spool piece at the top. This process is reversed to insert the cold finger, with a pause to evacuate the air out of the air lock and backfill with helium gas before opening the gate valve.

At the end of each safety test, the sample holder is typically analyzed for retained fission products. The tantalum container and tantalum tube that introduces sweep gas to the bottom of the container are also typically removed and analyzed, as these may also contain non-negligible amounts of metallic fission products that were not transported to the deposition cups.

The system is operated in a modular, walk-in hot cell at the IFEL, where the test apparatus can be installed on a campaign basis and removed as needed for maintenance. Fission gases released from the heated fuel are continually swept from the furnace by the helium gas stream and collected in the fission gas trap system, which includes two liquid nitrogen-cooled charcoal traps monitored with NaI detectors. The fission gas traps and detectors are located outside of the hot cell in a low background area to facilitate detection of very small quantities of ^{85}Kr. A photograph of the fission gas trap assembly is shown in Appendix Figure A-3. A diagram of one of the traps used prior to a redesign in 2017 is shown in Appendix Figure A-4, and Appendix Figure A-5 shows the redesigned trap. The redesigned traps have a charcoal collector module that can be removed from the vacuum insulated dewar and gamma detector shield assembly. This removable module allows for easy replacement of the charcoal should a high releasing experiment contaminate the trap with traces of nongaseous, volatile fission products, such as ^{134}Cs and ^{137}Cs.

* Text and figures in this appendix were extracted, with minor editing, from a previous milestone letter report (Morris and Baldwin 2010).

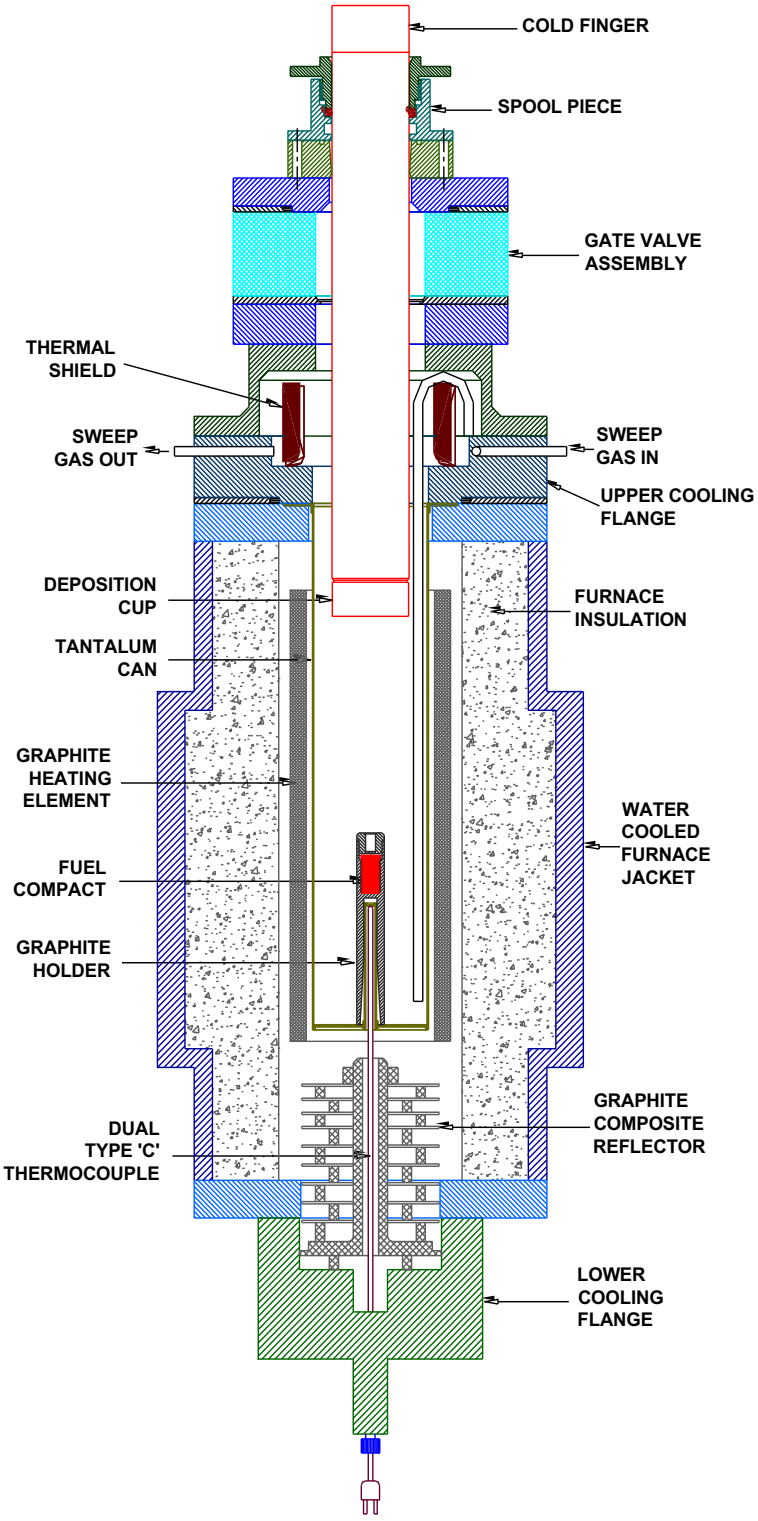

Appendix Figure A-1. Cross section of the CCCTF furnace.

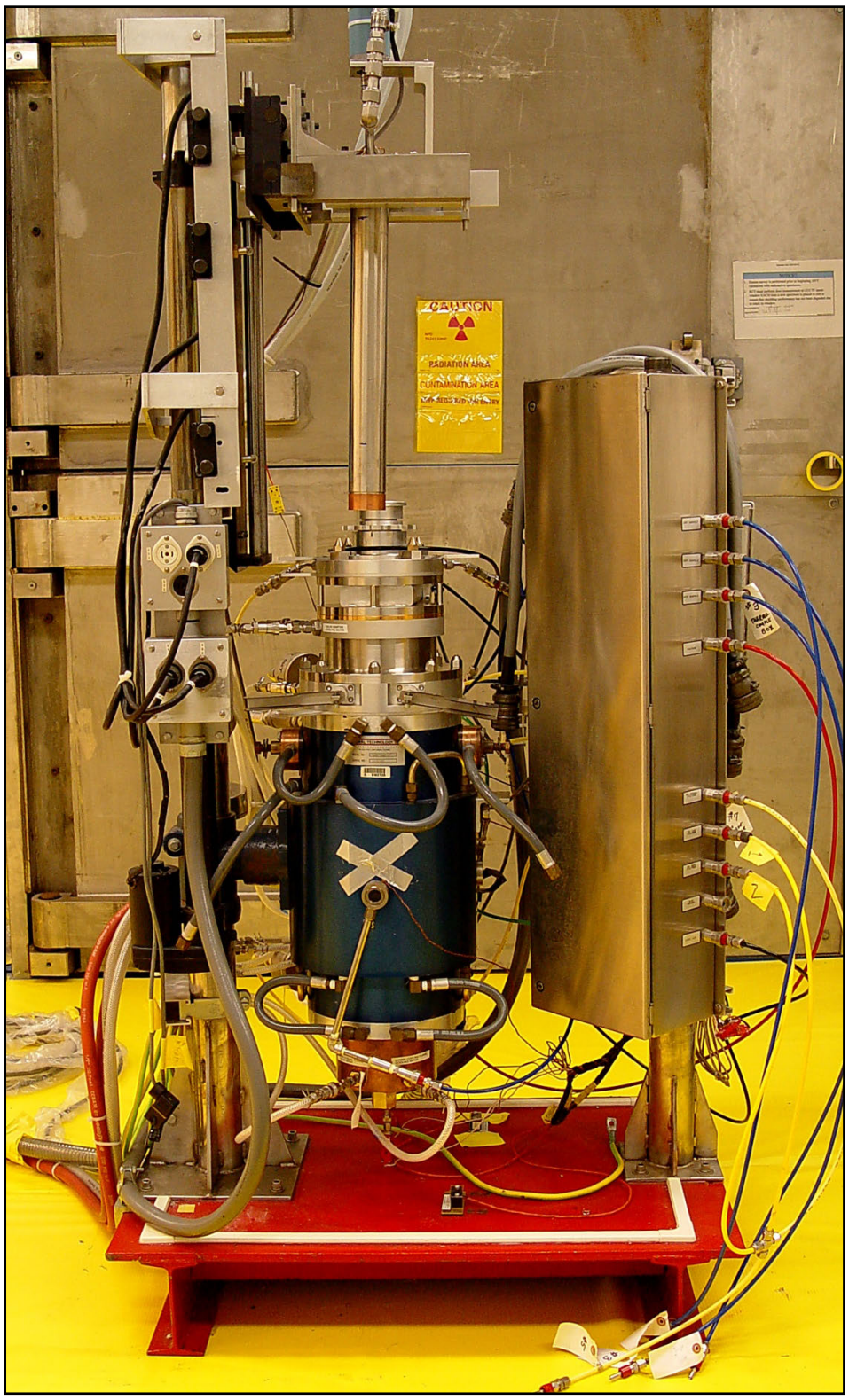

Appendix Figure A-2. CCCTF furnace in front of walk-in hood.

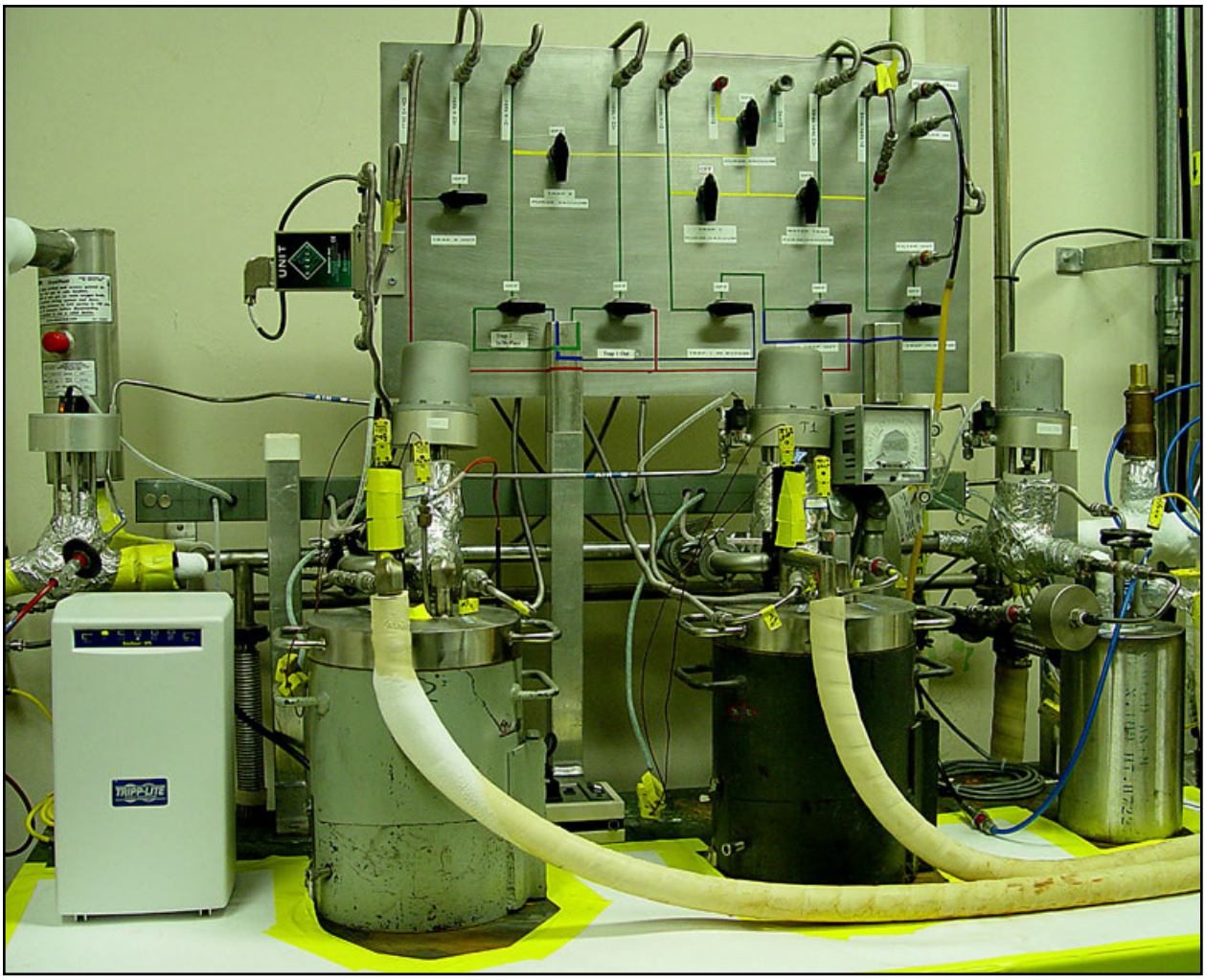

Appendix Figure A-3. CCCTF fission gas trap assembly.

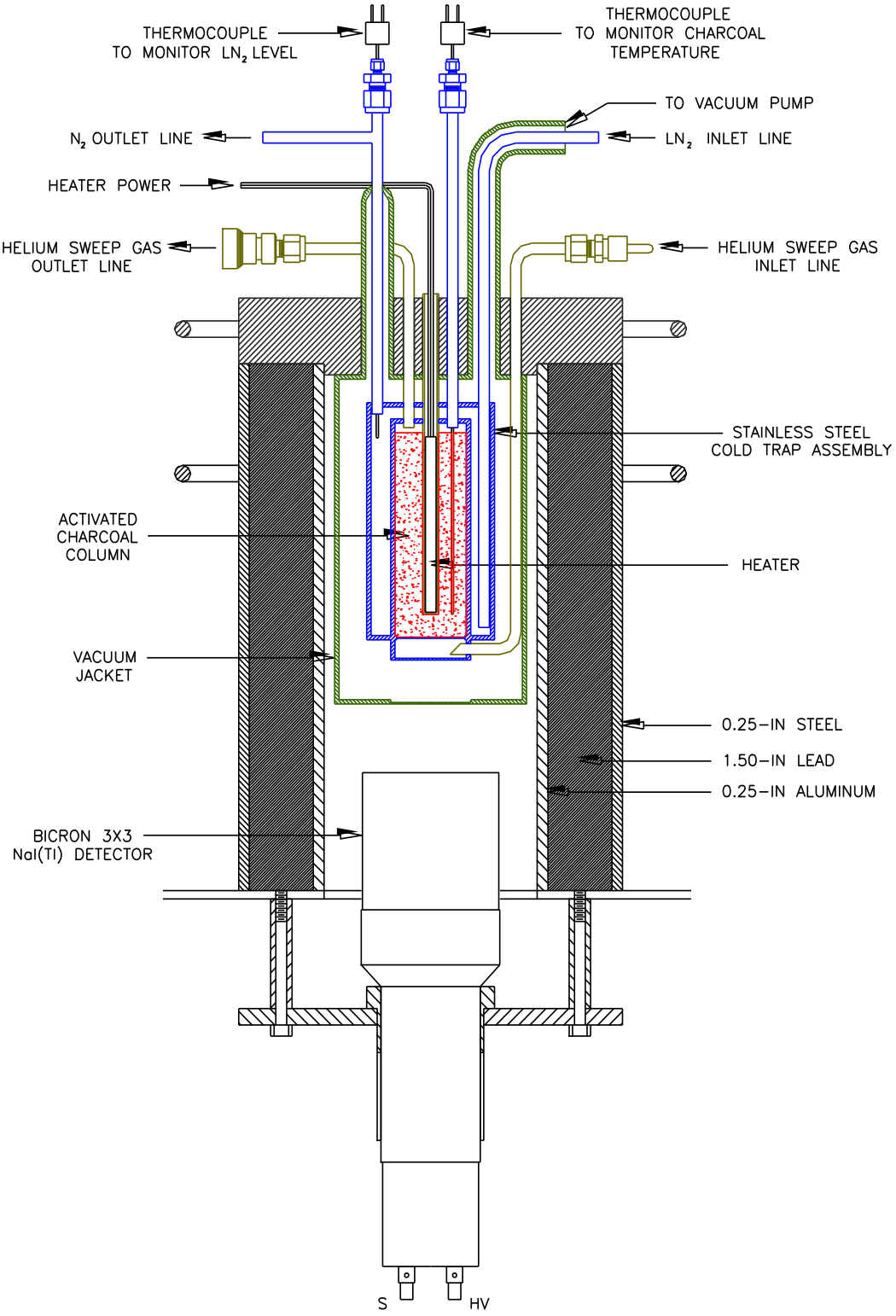

Appendix Figure A-4. Schematic of a liquid nitrogen-cooled charcoal trap before 2017 redesign.

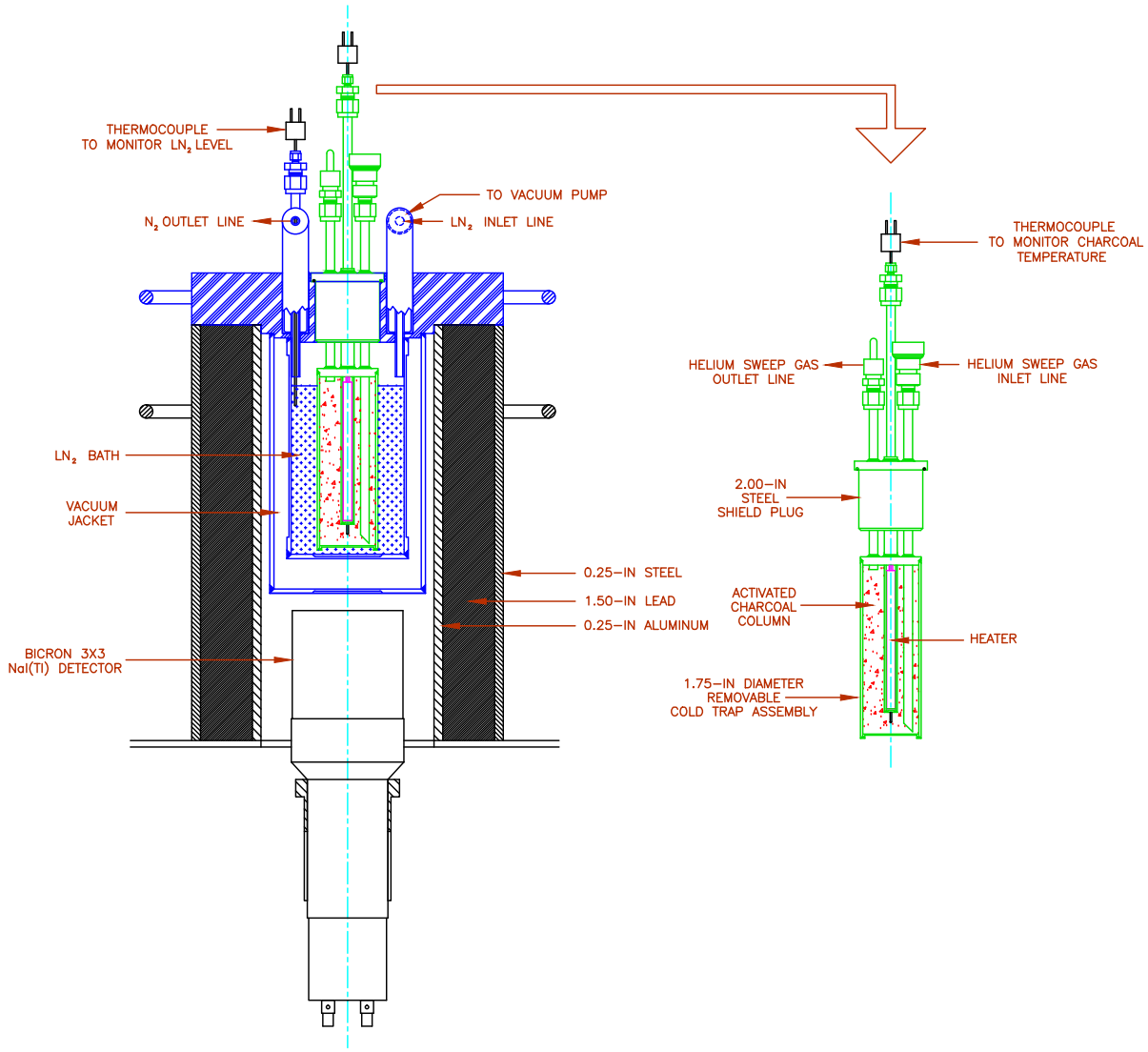

Appendix Figure A-5. Schematic of a liquid nitrogen-cooled charcoal trap after 2017 redesign.

APPENDIX B. CALCULATED INVENTORIES

The tables in this appendix provide the irradiated Compact 2-2-2 and 2-2-4 calculated inventories for radionuclides often measured during AGR program PIE and include those used herein. Calculated inventories in moles per compact were estimated via physics depletion calculations using the methods and input described by Sterbentz (Sterbentz 2020). Jim's MCNP-ORIGEN2 coupled utility program (JMOCUP) utilized the Oak Ridge Isotope Generation and Depletion (ORIGEN2) code (Croff 1983; Ludwig and Croff 2002) and the Monte Carlo N-Particle Transport (MCNP) code (X-5 Monte Carlo Team 2003). Note that these calculated inventories do not account for any possible transport of nuclides into or out of the fuel compacts during or after irradiation, they simply represent the net amount of each nuclide generated by the nuclear physics reactions occurring as a function of neutron interaction and time and not subsequently depleted by other nuclear physics reactions as of one day after EOI. The activity per particle was estimated from the activity per compact by multiplying by the reported average number of 2265 particles per compact (Pham et al. 2021).

Appendix Table B-1. Calculated inventories of select radionuclides one day after EOI

Compact	Value	^{85}Kr	^{90}Sr	^{106}Ru	^{110m}Ag	^{125}Sb
AGR-5/6/7 2-2-2	moles/compact	1.137E-06	2.481E-05	4.183E-06	1.236E-08	2.397E-07
AGR-5/6/7 2-2-2	Bq/compact	1.398E+09	1.140E+10	5.436E+10	2.391E+08	1.149E+09
AGR-5/6/7 2-2-2	Bq/particle	6.173E+05	5.033E+06	2.400E+07	1.056E+05	5.075E+05
AGR-5/6/7 2-2-4	moles/compact	1.157E-06	2.523E-05	4.385E-06	1.331E-08	2.473E-07
AGR-5/6/7 2-2-4	Bq/compact	1.423E+09	1.159E+10	5.698E+10	2.575E+08	1.186E+09
AGR-5/6/7 2-2-4	Bq/particle	6.282E+05	5.118E+06	2.516E+07	1.137E+05	5.235E+05

Appendix Table B-1 continued. Calculated inventories of select radionuclides one day after EOL

Compact	Value	^{134}Cs	^{137}Cs	^{144}Ce	^{154}Eu	^{155}Eu
AGR-5/6/7 2-2-2	moles/compact	3.182E-06	3.195E-05	9.786E-06	4.282E-07	1.557E-07
AGR-5/6/7 2-2-2	Bq/compact	2.038E+10	1.405E+10	1.659E+11	6.585E+08	4.333E+08
AGR-5/6/7 2-2-2	Bq/particle	8.998E+06	6.203E+06	7.326E+07	2.907E+05	1.913E+05
AGR-5/6/7 2-2-4	moles/compact	3.329E-06	3.266E-05	1.002E-05	4.447E-07	1.622E-07
AGR-5/6/7 2-2-4	Bq/compact	2.132E+10	1.436E+10	1.699E+11	6.839E+08	4.514E+08
AGR-5/6/7 2-2-4	Bq/particle	9.414E+06	6.341E+06	7.502E+07	3.019E+05	1.993E+05